Title

Let-7 Suppresses B Cell Activation through Restricting the Availability of Necessary Nutrients

Journal

Cell Metabolism, 27(2)

ISSN

1550-4131

Authors

Jiang, Shuai
Yan, Wei
Wang, Shizhen Emily
et al.

Publication Date

2018-02-01

DOI

10.1016/j.cmet.2017.12.007

Peer reviewed

Article

Cell Metabolism

Let-7 Suppresses B Cell Activation through Restricting the Availability of Necessary Nutrients

Graphical Abstract

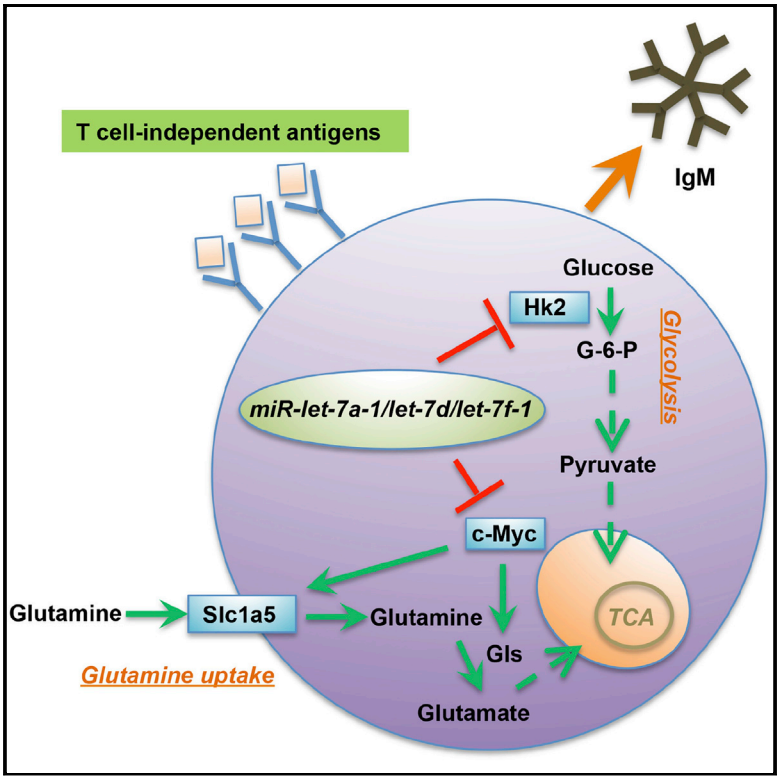

Highlights

- Overexpression or deletion of let-7adf leads to altered TI-IgM production in mice
- Let-7adf blocks biomass increase from principal nutrients in activated B cells
- Let-7adf directly targets *Hexokinase 2* (*Hk2*) and suppresses glycolysis
- Let-7adf suppresses glutamine uptake and utilization through regulating Myc

Authors

Shuai Jiang, Wei Yan,
Shizhen Emily Wang, David Baltimore

Correspondence

emilywang@ucsd.edu (S.E.W.),
baltimo@caltech.edu (D.B.)

In Brief

Activated B cells require nutrients to build biomass and function physiologically. Jiang et al. show that the microRNA let-7adf cluster acts as a "metabolic brake" in activated B cells by suppressing T cell-independent antigen-induced IgM antibody production. Mechanistically, let-7adf regulates uptake and utilization of key nutrients including glucose and glutamine.

Jiang et al., 2018, Cell Metabolism *27*, 393–403
February 6, 2018
https://doi.org/10.1016/j.cmet.2017.12.007

CellPress

Cell Metabolism
Article

Let-7 Suppresses B Cell Activation through Restricting the Availability of Necessary Nutrients

Shuai Jiang,[1,3] Wei Yan,[2,3] Shizhen Emily Wang,[2,*] and David Baltimore[1,4,*]
[1]Division of Biology and Biological Engineering, California Institute of Technology, Pasadena, CA 91125, USA
[2]Department of Pathology, University of California, San Diego, La Jolla, CA 92093, USA
[3]These authors contributed equally
[4]Lead Contact
*Correspondence: emilywang@ucsd.edu (S.E.W.), baltimo@caltech.edu (D.B.)
https://doi.org/10.1016/j.cmet.2017.12.007

SUMMARY

The control of uptake and utilization of necessary extracellular nutrients—glucose and glutamine—is an important aspect of B cell activation. Let-7 is a family of microRNAs known to be involved in metabolic control. Here, we employed several engineered mouse models, including B cell-specific overexpression of Lin28a or the let-7a-1/let-7d/let-7f-1 cluster (let-7adf) and knockout of individual let-7 clusters to show that let-7adf specifically inhibits T cell-independent (TI) antigen-induced immunoglobulin (Ig)M antibody production. Both overexpression and deletion of let-7 in this cluster leads to altered TI-IgM production. Mechanistically, let-7adf suppresses the acquisition and utilization of key nutrients, including glucose and glutamine, through directly targeting hexokinase 2 (Hk2) and by repressing a glutamine transporter Slc1a5 and a key degradation enzyme, glutaminase (Gls), a mechanism mediated by regulation of c-Myc. Our results suggest a novel role of let-7adf as a "metabolic brake" on B cell antibody production.

INTRODUCTION

Emerging evidence indicates that upon antigen encounter, B cells reprogram metabolism to meet the biosynthetic demands for antibody production (Capasso et al., 2015; Caro-Maldonado et al., 2014; Doughty et al., 2006; Le et al., 2012). Activation of B cells is accompanied by increased glycolysis and glutaminolysis (Buck et al., 2015; Caro-Maldonado et al., 2014; Dufort et al., 2007; Woodland et al., 2008). In order to build new biomass, activated B cells increase the import of necessary nutrients, such as glucose, and promote their utilization (Caro-Maldonado et al., 2014; Doughty et al., 2006). In addition to glucose, activated B cells need amino acids for synthesis of antibodies and other proteins, as well as nitrogen, for nucleotide synthesis and other processes (Calder, 2006; Grohmann and Bronte, 2010). As the most abundant amino acid in serum, glutamine is a readily available nutrient for most cells, and is involved in providing nitrogen for synthesis of many amino acids (Caro-Maldonado et al., 2014; Hensley et al., 2013). Several genes associated with amino acid transport and biosynthesis are induced under starvation conditions in various cell types, including B cells (Le et al., 2012; Shotwell et al., 1983). However, despite the fundamental role of necessary nutrients—glucose and glutamine—as building blocks for protein synthesis and substrates for multiple metabolic processes, regulation of uptake and utilization of these two key nutrients during B cell activation is incompletely understood.

MicroRNAs (miRNAs) play critical roles in multiple biological processes and diseases, including metabolism, immunity, and cancer (Baltimore et al., 2008; Rottiers and Naar, 2012; So et al., 2013). However, much remains to be learned about their physiological roles. The let-7 miRNA family, initially identified as a regulator of developmental timing in *Caenorhabditis elegans,* consists of 12 members expressed from eight genomic loci in mice (let-7a-1, let-7a-2, let-7b, let-7c-1, let-7c-2, let-7d, let-7e, let-7f-1, let-7f-2, let-7g, let-7i, and miR-98), all of which share the same "seed sequence" (Reinhart et al., 2000; Su et al., 2012). The let-7a-1/let-7d/let-7f-1 cluster (denoted as let-7adf cluster), with three members let-7a-1, let-7f-1, and let-7d, is an important cluster of the let-7 family, accounting for about 25% of total let-7 precursors (Wang et al., 2011). Studies using various mouse models of cancer indicate that let-7 usually inhibits tumor growth in adult mice (Esquela-Kerscher et al., 2008; Hu et al., 2013; Wu et al., 2015). A handful of previous studies have also implicated let-7 in the regulation of glucose metabolism and amino acid sensing (Boyerinas et al., 2010; Dubinsky et al., 2014; Jiang and Baltimore, 2016; Nguyen and Zhu, 2015; Zhu et al., 2011). However, relatively little is known about the physiological role of a single let-7 cluster in the adaptive immune system, for instance in the regulation of *in vivo* B cell function.

While the molecular mechanisms controlling the availability of nutrients to support B cell function remain to be characterized, the let-7 family of miRNAs has been shown to control puberty and growth in mice by regulating glucose metabolism (Zhu et al., 2011), and can regulate the bioenergetic state during tissue repair *in vivo* (Shyh-Chang et al., 2013). These prior studies linking let-7 to metabolic regulation suggested to us that let-7 might regulate the capacity of B cells to produce antibody

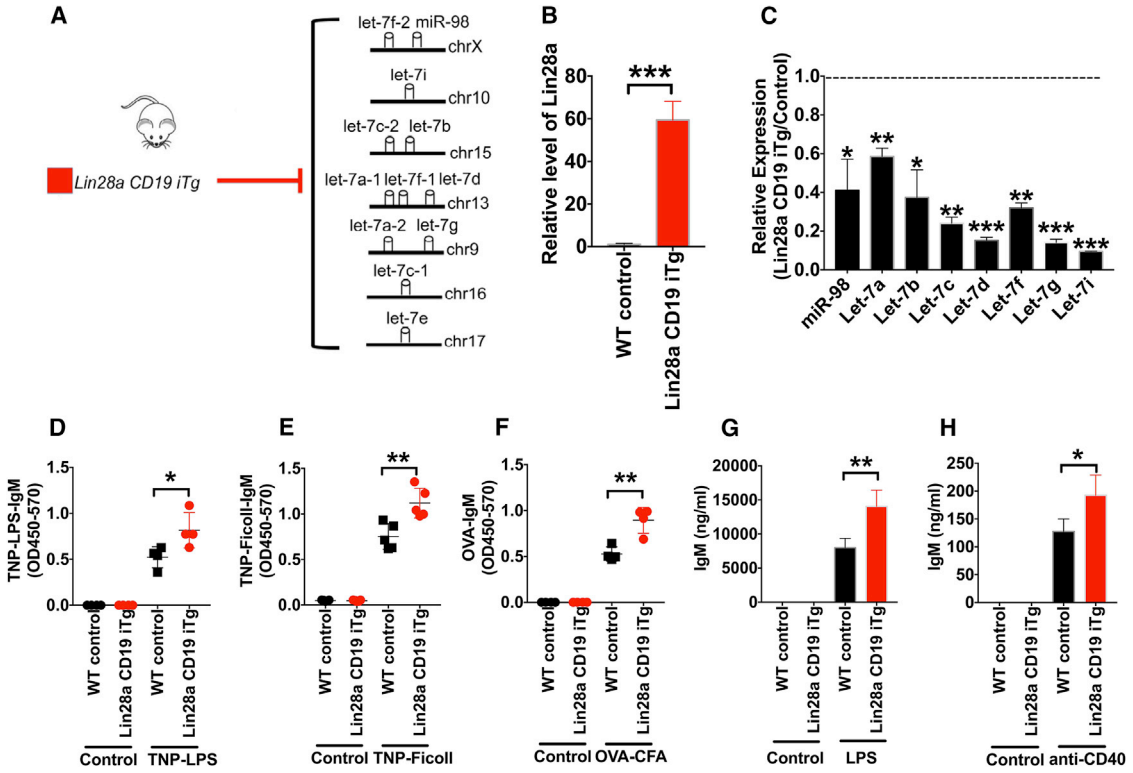

Figure 1. Comprehensive Repression of All let-7 miRNAs Enhances IgM Production *In Vivo*

(A) Schema indicating the repression of entire let-7 miRNA family in CD19 Cre-inducible Lin28a expression mice (Lin28a iTg).

(B) Lin28a expression is induced in splenic B cells. Quantitative RT-PCR was performed using RNA isolated from purified splenic B cells.

(C) Lin28a overexpression suppresses let-7 expression in B cells.

(D) Quantification of TNP-LPS-specific IgM in the serum of Lin28a iTg mice and control WT mice 7 days after TNP-LPS immunization.

(E) Quantification of TNP-FicoII-specific IgM production in the serum of Lin28a iTg mice and control WT mice 7 days after TNP-FicoII immunization.

(F) Quantification of OVA-specific IgM production in the serum of Lin28a iTg mice and control WT mice 21 days after OVA immunization.

(G) Purified murine B cells were cultured in medium alone to maintain viability or stimulated with LPS and ELISA for IgM secretion after 7 days.

(H) Purified murine B cells were cultured in medium alone to maintain viability or stimulated with anti-CD40 and ELISA for IgM secretion after 7 days.

*$p < 0.05$, **$p < 0.01$, and ***$p < 0.001$ using Student's t test.

through modulating the metabolic reprogramming events associated with this immune function.

To elucidate the physiological function of let-7 in mammals, we first studied in mice the overall inhibition of all let-7 members mediated by B cell-specific overexpression of the protein Lin28a and found increased immunoglobulin (Ig)M production. Specific deletion of the let-7adf cluster in mice resulted in enhanced T cell-independent (TI) antigen-induced IgM production, whereas B cell-specific overexpression of the let-7adf cluster had the opposite effect. Mechanistically, we found that the let-7adf cluster inhibited the uptake and utilization of both glucose and glutamine in activated B cells. The let-7adf cluster regulated glycolysis through directly targeting *Hk2*. We also found that the same let-7 cluster repressed glutaminolysis by simultaneously regulating *Slc1a5* and *Gls* through regulating *c-Myc*. Thus, we show that the let-7adf cluster specifically suppresses TI antigen-induced IgM production in B cells by preventing the uptake and usage of necessary nutrients, acting as a brake on the extent of B cell activation and antibody production following antigen stimulation. The let-7adf cluster thereby plays a previously unappreciated mediating role in B cell biology.

RESULTS

Comprehensive Repression of All let-7 miRNAs Enhances IgM Production *In Vivo*

To first determine the effect of global repression of all let-7 miRNAs on B cell function *in vivo*, we crossed transgenic mice carrying the inactive transgene construct (Lin28a Tg OFF) with those expressing CD19-Cre to generate B cell-specific CD19-Cre-dependent Lin28a transgenic mice (denoted as Lin28a CD19 iTg) (Figure 1A). Lin28a CD19 iTg mice did not show an overt pathology compared with wild-type (WT) littermates (data not shown). In this system, Lin28a is specifically expressed from the B cell-specific CD19 promoter, with an overexpression of about 60-fold in splenic B cells (Figure 1B). The overall levels of let-7 family members were significantly but incompletely decreased in Lin28a iTg B cells (Figure 1C), consistent with the known function of Lin28a to suppress mature let-7 miRNAs. To examine the *in vivo* effect of Lin28a overexpression on B cell antibody production, we first challenged the Lin28a CD19 iTg mice with TI antigens (2,4,6-trinitrophenyl [TNP]-lipopolysaccharide [LPS] and TNP-Ficoll). Analysis of TNP-specific IgM production demonstrated

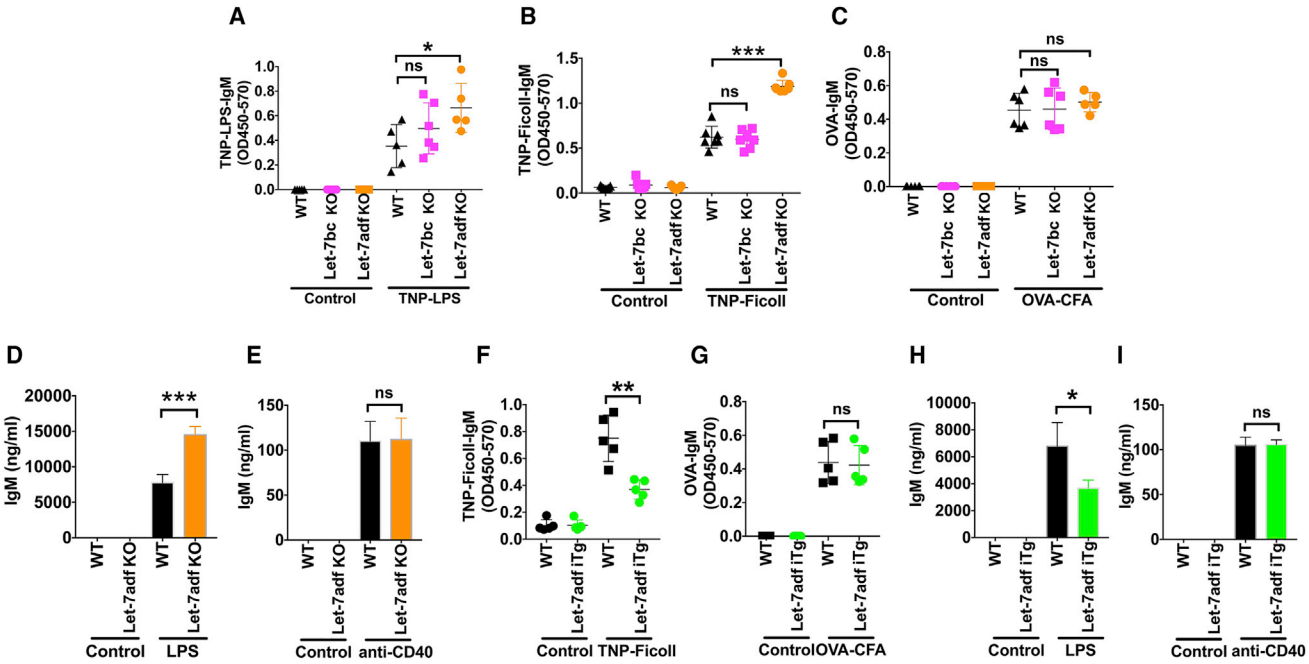

Figure 2. The let-7a-1/let-7d/let-7f-1 Cluster Is a Critical Regulator of TI Antigen-Induced IgM Production in Mice

(A) Quantification of TNP-LPS-specific IgM in the serum of the let-7adf cluster KO mice, the let-7bc cluster KO mice, and control WT mice 7 days after TNP-LPS immunization.

(B) Quantification of TNP-Ficoll-specific IgM production in the serum of the let-7adf cluster KO mice, the let-7bc cluster KO mice, and control WT mice 7 days after TNP-Ficoll immunization.

(C) Quantification of OVA-specific IgM production in the serum of the let-7adf cluster KO mice, the let-7bc cluster KO mice, and control WT mice 21 days after OVA immunization.

(D) Purified murine B cells from the let-7adf cluster KO mice and WT control mice were cultured in medium alone to maintain viability or stimulated with LPS and ELISA for IgM secretion after 7 days.

(E) Purified murine B cells from the let-7adf cluster KO mice and WT control mice were cultured in medium alone to maintain viability or stimulated with anti-CD40 and ELISA for IgM secretion after 7 days.

(F) Quantification of TNP-Ficoll-specific IgM in the serum of the let-7adf cluster CD19 iTg mice, and control WT mice 7 days after TNP-Ficoll immunization.

(G) Quantification of OVA-specific IgM production in the serum of the let-7adf cluster iTg mice, and control WT mice 21 days after OVA immunization.

(H) Purified murine B cells from the let-7adf cluster CD19 iTg mice and WT control mice were cultured in medium alone to maintain viability or stimulated with LPS and ELISA for IgM secretion after 7 days.

(I) Purified murine B cells from the let-7adf cluster iTg mice and WT control mice were cultured in medium alone to maintain viability or stimulated with anti-CD40 and ELISA for IgM secretion after 7 days.

*$p < 0.05$, **$p < 0.01$, and ***$p < 0.001$ using Student's t test; ns, not significant.

that Lin28a overexpression significantly promoted both TI-1 and TI-2 antigen-induced IgM production *in vivo* (Figures 1D and 1E). This partial enhancement of IgM production was in line with an increased response to ovalbumin (OVA)-CFA, a T cell-dependent (TD) antigen challenge, where we observed that ectopic expression of Lin28a increased OVA-specific IgM production (Figure 1F). Thus, comprehensive let-7 family repression enhanced both TI and TD antigen-induced IgM production *in vivo*.

To further confirm the effect of Lin28a overexpression on antibody production *in vitro*, we treated B cells isolated from the Lin28a CD19 iTg or WT mice with LPS, mimicking a TI antigen challenge, and found that Lin28a overexpression caused increased IgM production (Figure 1G). Following anti-CD40 treatment, mimicking a TD antigen challenge *in vitro*, we also observed enhanced IgM production in Lin28a iTg B cells (Figure 1H). Collectively, our results show that comprehensive repression of the entire let-7 family through Lin28a overexpression enhances antibody production *in vivo* and *in vitro*.

The let-7a-1/let-7d/let-7f-1 Cluster Is a Critical Regulator of TI Antigen-Induced IgM Production in Mice

To confirm that the effect observed in the Lin28a overexpression model is mediated by let-7 miRNAs, and to further address whether single let-7 clusters played individual or redundant roles in this regard, we performed *in vivo* antigen challenges in additional transgenic mouse models with let-7 manipulations. We first examined mice with a genetic knockout (KO) of the let-7adf cluster (Figure S1A) or the let-7b/let-7c-2 cluster (denoted as let-7bc cluster) following TI antigen challenge with TNP-LPS or TNP-Ficoll. We found that deletion of the let-7adf cluster significantly enhanced both TI-1 and TI-2 antigen-specific IgM production, whereas deletion of the let-7bc cluster had no significant effect (Figures 2A and 2B), indicating that the let-7adf cluster plays a specific role in the regulation of TI antigen-induced IgM production.

To further determine whether these two clusters affected TD antigen-induced IgM production, we examined OVA-CFA-induced IgM production in both KO mice. We found that neither

gene cluster deletion affected TD antigen-induced IgM production (Figure 2C). These results demonstrate that the let-7adf cluster specifically blocks TI, but not TD, antigen-induced IgM production *in vivo*. Next, we examined IgM production in the let-7adf cluster KO B cells following LPS and anti-CD40 treatment *in vitro*, and we found that IgM production following LPS stimulation, but not anti-CD40 treatment, was significantly enhanced by deletion of the let-7adf cluster (Figures 2D and 2E).

To investigate the converse—if ectopic expression of the let-7adf cluster in B cells impairs TI antigen-induced antibody production *in vivo*—we generated transgenic mice that expressed the let-7adf cluster in a B cell-specific manner (under CD19 control) (denoted as let-7adf iTg; Figure S1B), and challenged these mice and controls with TNP-Ficoll. The transgenic mice showed impaired TNP-specific IgM production compared with WT mice, confirming that the let-7adf cluster functions to block TI antigen-induced IgM antibody production (Figure 2F). As expected, we did not observe any difference of OVA-specific IgM production in let-7adf iTg mice, compared with WT mice (Figure 2G), further confirming that the let-7adf cluster is dispensable to TD antigen-induced IgM production *in vivo*. To test whether the let-7adf cluster affected TI antigen-induced IgM production *in vitro*, we treated let-7adf iTg B cells with LPS and found that overexpression of the let-7adf cluster indeed suppressed IgM production *in vitro* (Figure 2H), but not for anti-CD40-induced IgM production (Figure 2I). Collectively, these results indicate that the let-7adf cluster plays a physiological role of suppressing TI antigen-induced IgM antibody production *in vitro* and *in vivo*. We also observed that the expression of let-7a, let-7d, and let-7f was upregulated 24 hr after LPS treatment, compared with non-activated B cells (Figure S1C), suggesting that the LPS induction of these miRNAs may help tailor the B cell immune responses to TI antigens and the upregulation of let-7a, let-7d, and let-7f by activation may be a feedback mechanism for dampening the B cell immune response.

The let-7a-1/let-7d/let-7f-1 Cluster Inhibits Glycolytic Capacity and Glucose Uptake without Significantly Affecting Mitochondrial Respiration in B Cells

Altered B cell metabolism during antibody production has been reported (Caro-Maldonado et al., 2014). To examine the possibility that the let-7adf cluster might contribute to the regulation of B cell metabolism, we measured glycolysis, using the Seahorse Extracellular Flux analyzer to examine the extracellular acidification rate (ECAR) in the let-7adf cluster KO B cells following 6 hr of LPS stimulation. The ECAR curve was higher in let-7adf cluster KO B cells than in WT B cells (Figure 3A, left). The glycolytic capacity, the maximum rate of conversion of glucose to pyruvate or lactate, was higher in KO B cells compared with WT B cells (Figure 3A, right). Compared with LPS-activated B cells, our ECAR measurements in unstimulated B cells did not show any difference between let-7adf KO and WT B cells (Figure 3B), indicating that the effect of let-7adf on ECAR occurs only following stimulation.

To next determine whether the let-7adf cluster also regulates mitochondrial respiration, we measured mitochondrial oxygen consumption rate (OCR), an indicator of mitochondrial respiration, and found that the OCR curve was unchanged in the let-7adf cluster KO B cells compared with WT B cells (Figure 3C), and some key respiratory flux parameters, such as basal OCR and ATP-linked OCR, determined by the basal measurement minus oligomycin response, as well as maximal oxygen consumption rates, were comparable between the let-7adf cluster KO B cells and WT B cells (data not shown), indicating the let-7adf cluster is not regulating B cell respiratory capacity. We did not observe any significant differences in the OCR curve between the let-7adf cluster KO B cells and WT B cells (Figure 3D), suggesting that the effect of let-7adf on OCR also happens only following stimulation.

We next examined whether the let-7adf cluster affected B cell ECAR in B cells from the let-7adf iTg mice. Conversely to the KO model, cells with overexpression of the gene cluster had a markedly attenuated ECAR curve (Figure 3E, left) and a lower glycolytic capacity compared with WT B cells (Figure 3E, right). Mitochondrial respiration was not affected by overexpressing the let-7adf cluster (Figure 3F). These data demonstrated that the let-7adf cluster functions to restrict the glycolytic capacity in B cells without affecting oxidative respiratory capacity. To examine the possibility that let-7adf might have an impact on B cell proliferation, we measured cell proliferation and found no effect (data not shown), thus implying that the effects shown in Figures 3A and 3E are not due to differences in cell proliferation. To further test whether let-7adf directly affected glucose uptake, we examined B cell glucose uptake and found that let-7adf KO B cells have enhanced glucose uptake compared with WT B cells (Figure 3G), while let-7adf iTg B cells have reduced glucose uptake compared with WT control B cells (Figure 3H), indicating that let-7adf represses B cell glucose uptake. In addition, we observed enhanced Glut1 expression in let-7adf KO B cells (Figures S2A and S2B), indicating that the let-7adf cluster regulates glucose uptake in activated B cells.

Hexokinase II Is a Direct Target of the let-7a-1/let-7d/let-7f-1 Cluster and Promotes B Cell Glycolysis

To further investigate the underlying mechanism through which the let-7adf cluster regulates glycolysis in B cells, we screened for messenger RNAs with 3′ untranslated regions (UTRs) that could be putative targets of let-7d, using the TargetScan algorithm predictions (Agarwal et al., 2015). We identified *Hk2* and *Pdk1 (pyruvate dehydrogenase kinase 1),* critical enzymes in the glycolysis pathway, as potential targets of let-7d in B cells (Figure 4A; only the *Hk2* 3′ UTR is shown). To study the regulation of these two glycolytic genes by let-7d in B cells, we assayed protein and mRNA expression levels of both Hk2 and Pdk1 in let-7d KO B cells. RT-PCR and western blot analyses showed that Hk2 mRNA and protein levels were dramatically enhanced in the let-7adf cluster KO B cells (Figures 4B and 4C), indicating that *Hk2* might be a direct target of the let-7adf cluster in B cells. We also found that Hk2 mRNA and protein levels were decreased in the B cells of the let-7adf cluster CD19 iTg mice compared with WT controls (Figures 4D and 4E). However, we did not observe a significant difference in the expression of Pdk1 between the let-7adf cluster KO and WT B cells (Figures S2C and S2D), indicating that Pdk1 is not a target of let-7d in B cells, consistent with the observation that the let-7adf cluster inhibits glycolysis in B cells without affecting oxidative respiratory capacity.

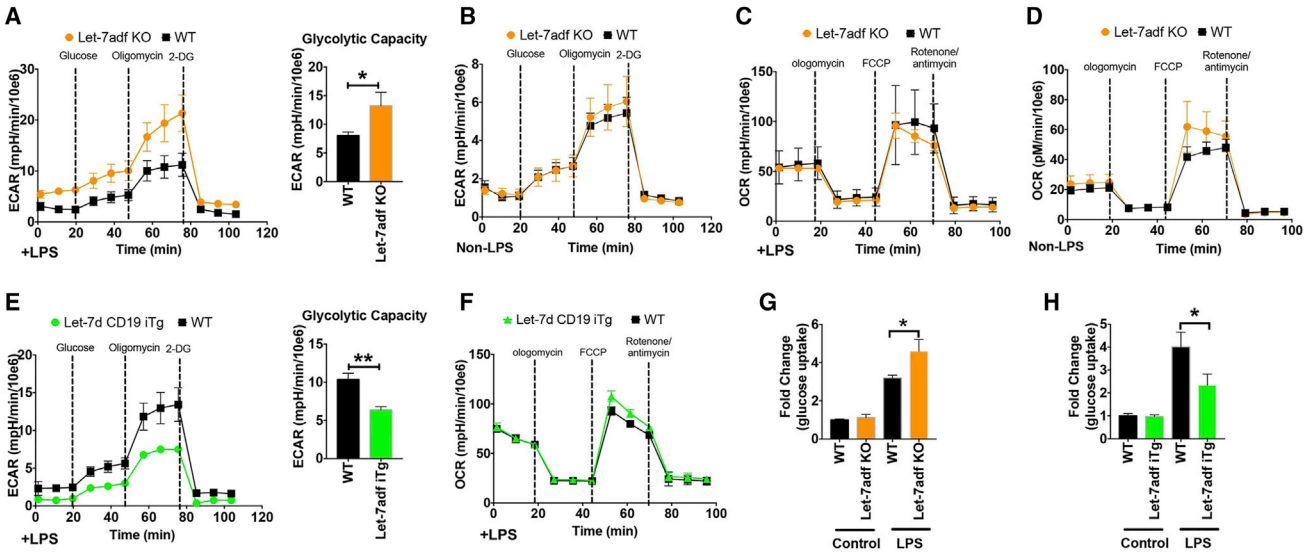

Figure 3. The let-7a-1/let-7d/let-7f-1 Cluster Inhibits Glycolytic Capacity and Glucose Uptake without Significantly Affecting Mitochondrial Respiration in B Cells

(A and B) Purified the let-7adf cluster KO and WT B cells were examined after 6 hr of culture with LPS (A) or without LPS treatment (B), and ECAR was determined by extracellular flux analysis. A representative plot of ECAR over time of B cells with addition of glucose (10 mM), oligomycin (1 μM), and 2-DG (50 mM) as indicated (A, left, and B); glycolytic capacity of LPS-treated KO/WT B cells (A, right).

(C and D) Purified let-7adf cluster KO and WT B cells were examined after 6 hr culture with LPS (C) or without LPS treatment (D), and OCR was determined by extracellular flux analysis. A representative plot of OCR over time with addition of oligomycin (1 μM), mitochondrial uncoupler p-trifluoromethoxy carbonyl cyanide phenyl hydrazine (FCCP) (0.5 μM), and electron transport inhibitors antimycin (1.5 μM) + rotenone (0.75 μM), as indicated.

(E) Purified the let-7adf cluster iTg and WT B cells were examined after 6 hr of culture with LPS, and ECAR was determined by extracellular flux analysis. A representative plot of ECAR over time of B cells with addition of glucose (10 mM), oligomycin (1 μM), and 2-DG (50 mM), as indicated (E, left); glycolytic capacity of LPS-treated iTg/WT B cells (E, right).

(F) Purified the let-7adf cluster iTg and WT B cells were examined after 6-hr culture with LPS, and OCR was determined by extracellular flux analysis. A representative plot of OCR over time with addition of oligomycin (1 μM), mitochondrial uncoupler FCCP (0.5 μM), and electron transport inhibitors antimycin (1.5 μM) + rotenone (0.75 μM), as indicated.

(G) Fold change of glucose uptake in the non-LPS- and LPS-treated B cells from the let-7adf cluster KO mice and WT control mice.

(H) Fold change of glucose uptake in the non-LPS- and LPS-treated B cells from the let-7adf cluster iTg mice and WT control mice.

*$p < 0.05$ and **$p < 0.01$ using Student's t test.

Next, we directly examined the effect of let-7d by transfecting HEK293T cells with a chemically modified double-stranded RNA let-7d mimic in the presence of a luciferase reporter immediately upstream of either the WT 3′ UTR of Hk2 or one with a mutated let-7d binding site. Compared with the control, let-7d mimic significantly inhibited the expression of luciferase gene with an intact Hk2 3′ UTR, whereas with a mutated let-7d-binding site, there was unrestrained luciferase expression in the presence of let-7d (Figure 4F). Although it is known that Hk2—as the rate-limiting enzyme directly activating glucose to be a glycolysis substrate by phosphorylating glucose to glucose 6-phosphate—plays an important role in enhancing glycolysis in cancer cells (Mathupala et al., 2006), the functional role of Hk2 in B cells has not previously been addressed. To further test whether targeting *hk2* is one of the mechanisms that was involved in let-7adf-mediated IgM production and glucose uptake, the HK2 transcript was overexpressed in let-7adf iTg B cells, and we found that it rescued the effect of let-7adf overexpression on IgM production and glucose uptake (Figures 4G and 4H).

Taken together, our results show that an activator of B cells causes an increased production of the let-7adf cluster that inhibits the uptake and utilization of glucose in activated B cells, limiting the strength of activation.

The let-7a-1/let-7d/let-7f-1 Cluster Represses B Cell Glutamine Uptake and Utilization by Regulating the Glutamine Transporter Slc1a5 and Gls

To further examine whether the let-7adf cluster also regulates other metabolic pathways, we monitored the intracellular metabolite levels by one-dimensional nuclear magnetic resonance spectroscopy (1D nuclear magnetic resonance [NMR]). We found that the abundance of lactate was dramatically increased in the let-7adf cluster KO B cells compared with WT B cells, further supporting our observations of an enhanced ECAR and increased Hk2 expression in these genetically modified cells. In addition, we also observed enhanced levels of glutamate, as well as a higher level of ATP/ADP, in the let-7adf cluster KO B cells (Figures S3A–S3C), indicating a potential regulatory effect of the let-7adf cluster on glutaminolysis.

To test whether the increased intracellular level of glutamate in the let-7adf cluster KO B cells was derived from glucose feeding into amino acid synthesis as a result of enhanced glycolysis, or as a direct result of enhanced glutamine uptake, we performed

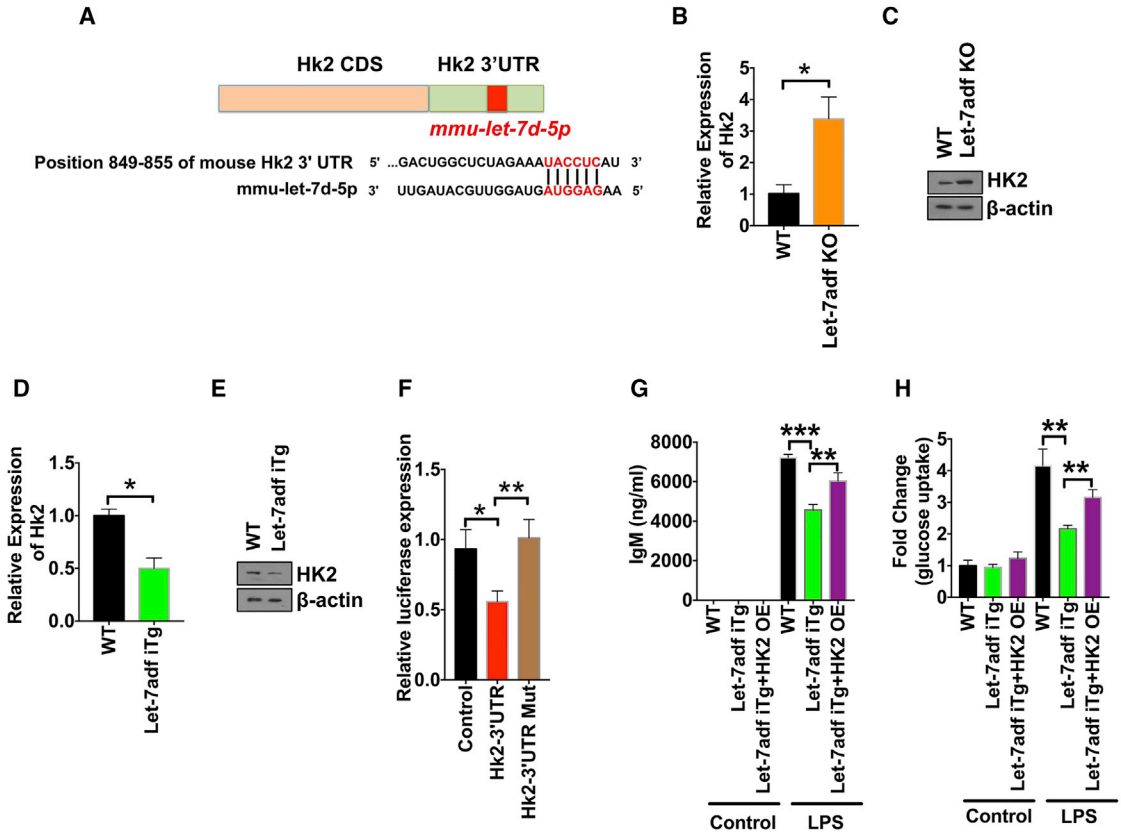

Figure 4. Hexokinase II Is a Direct Target of the let-7a-1/let-7d/let-7f-1 Cluster and Promotes B Cell Glycolysis

(A) Schematic of the predicted let-7d binding site in the Hk2 3′ UTR.

(B) The mRNA expression by qRT-PCR of Hk2 in WT control or the let-7adf cluster KO B cells.

(C) Hk2 protein expression in B cells from WT or the let-7adf cluster KO mice obtained by western blot.

(D) The mRNA expression by qRT-PCR of Hk2 in control or the let-7adf cluster iTg B cells.

(E) Hk2 protein expression in B cells from WT or the let-7adf cluster iTg mice obtained by western blot.

(F) Hk2 3′ UTR luciferase reporter assays in HEK293T cells.

(G) Purified murine B cells from the let-7adf cluster CD19 iTg mice and WT control mice, and let-7adf iTg B cells overexpressed with HK2 were cultured in medium alone to maintain viability or stimulated with LPS and ELISA for IgM secretion after 7 days.

(H) Fold change of glucose uptake in the non-LPS and LPS-treated B cells from the let-7adf cluster iTg mice and WT control mice and let-7adf iTg B cells overexpressed with HK2.

*$p < 0.05$, **$p < 0.01$, and ***$p < 0.001$ using Student's t test.

metabolic tracing by 2D NMR in cells treated with ^{13}C-labeled glucose. Consistent with other results, increased levels of ^{13}C-containing lactate were detected in the let-7adf cluster KO cells compared with WT B cells, but the levels of ^{13}C-labeled glucose-derived glutamate was only modestly altered (Figures S4A and S4B). These results suggest that the enhanced glutamate level in the let-7adf cluster KO B cells was not a result of altered glucose metabolism but might be dependent on glutaminolysis.

We therefore analyzed the glutamine consumption and glutamate production using the conditioned medium from LPS-treated B cells. We observed that the consumption of glutamine as well as the production of glutamate and ammonium were all increased in the let-7adf cluster KO B cells (Figures 5A–5C), suggesting that in WT cells, the let-7adf cluster is partially repressing B cell glutaminolysis. Moreover, metabolic tracing of ^{13}C-labeled glutamine analyzed by 2D NMR showed enhanced glutaminolysis, indicated by increased ^{13}C-labeled glutamine-derived glutamate in the let-7adf cluster KO B cells (Figure S5C), confirming that the let-7adf cluster also regulated glutaminolysis in B cells.

Let-7f has been reported to repress the glutamine transporter ASCT2 (*Slc1a5*), suppressing the mTORC1 pathway and inducing autophagy in neurons (Dubinsky et al., 2014). The high-affinity glutamine transporter Slc1a5 is rapidly elevated at both the mRNA and protein levels following lymphocyte stimulation (Nakaya et al., 2014). We therefore examined whether the let-7adf cluster affected glutamine uptake and glutamine consumption by regulating *Slc1a5*. As expected, we found that both mRNA and protein levels of *Slc1a5* were increased in the let-7adf cluster KO B cells (Figures 5D and 5F). We also found that the expression of glutaminase (*Gls*), a key enzyme in glutamine utilization, was enhanced in the let-7adf cluster KO B cells (Figures 5E and 5F). In contrast, we observed a converse effect—lower glutamine uptake and utilization in let-7adf iTg B cells compared with WT

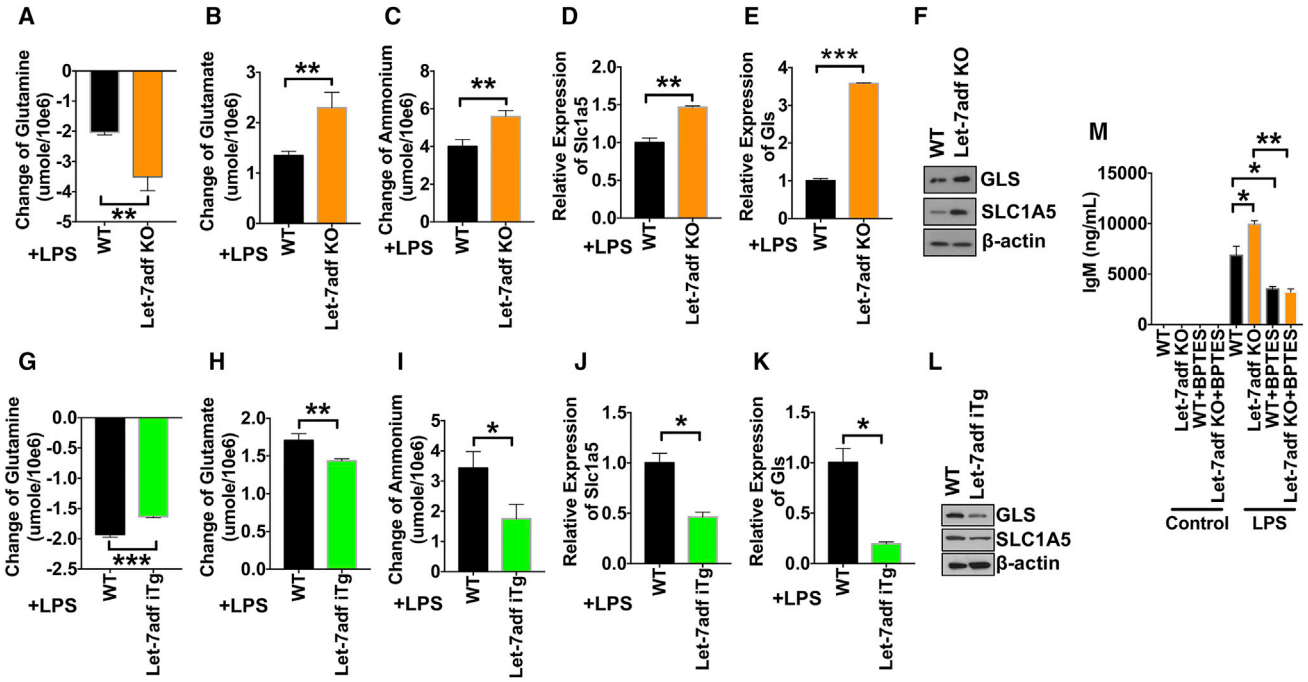

Figure 5. The let-7a-1/let-7d/let-7f-1 Cluster Represses B Cell Glutamine Uptake and Utilization by Regulating Glutamine Transporter Slc1a5 and Gls

(A) Quantification of glutamine uptake in WT or the let-7adf cluster KO B cells activated by LPS.
(B) Quantification of glutamate production in WT or the let-7adf cluster KO B cells activated by LPS.
(C) Quantification of ammonium production in WT or the let-7adf cluster KO B cells activated by LPS.
(D) mRNA expression determined by qRT-PCR of Gls in WT or the let-7adf cluster KO B cells.
(E) mRNA expression determined by qRT-PCR of Slc1a5 in WT or the let-7adf cluster KO B cells.
(F) The Slc1a5 and Gls protein expression in B cells from WT or the let-7adf cluster KO mice obtained by western blot.
(G) Quantification of glutamine uptake in WT or the let-7adf cluster iTg B cells activated by LPS.
(H) Quantification of glutamate production in WT or the let-7adf cluster iTg B cells activated by LPS.
(I) Quantification of ammonium production in WT or the let-7adf cluster iTg B cells activated by LPS.
(J) mRNA expression determined by qRT-PCR of Gls in WT or the let-7adf cluster iTg B cells.
(K) mRNA expression determined by qRT-PCR of Slc1a5 in WT or the let-7adf cluster iTg B cells.
(L) The Slc1a5 and Gls protein expression in B cells from WT or the let-7adf cluster iTg mice obtained by western blot.
(M) LPS- or non-LPS-treated purified murine B cells from the let-7adf cluster KO mice and WT control mice were cultured in medium stimulated with BPTES for IgM secretion after 7 days.
*p < 0.05, **p < 0.01, and ***p < 0.001 using Student's t test.

control B cells (Figures 5G–5L). In the presence of BPTES, the inhibitor of glutaminase, we found that it could counteract the induced IgM antibody production by let-7adf (Figure 5M), confirming that let-7adf cluster represses IgM production partially by regulating the glutamine utilization pathway.

Together, our data suggested that the let-7adf cluster inhibits B cell glutamine uptake and utilization by coordinately repressing *Slc1a5* and *Gls*.

The let-7a-1/let-7d/let-7f-1 Cluster Represses Glutamine Uptake and Utilization by Regulating c-Myc in B Cells

c-Myc has been shown to enhance both mitochondrial glutaminase expression and glutamine metabolism, and it can promote the expression of glutamine transporter Slc1a5 in human B lymphoma cells P493-6 at the transcriptional level (Caro-Maldonado et al., 2014; Gao et al., 2009). Moreover, a double-negative feedback loop between let-7 and c-Myc has been well established (Kolenda et al., 2014; Sampson et al., 2007; Wagner et al., 2014; Wang et al., 2012). Therefore, to further investigate the mechanism of the let-7adf cluster in regulating the uptake and utilization of glutamine in activated B cells, we examined the expression of c-Myc in the let-7adf cluster KO B cells. We found that the mRNA and protein levels were increased in the let-7adf cluster KO B cells compared with WT (Figures 6A and 6B), indicating that the let-7adf cluster might modulate the uptake and utilization of glutamine by regulating c-Myc in B cells. Furthermore, we observed that the mRNA and protein levels of c-Myc were dramatically decreased in the let-7afd cluster iTg B cells (Figures 6C and 6D), further supporting the presence of a let-7/c-Myc regulatory axis in B cells. To further test whether the let-7adf cluster regulates the uptake and utilization of glutamine by modulating c-Myc, we used the small-molecule c-Myc inhibitor 10058-F4 to block c-Myc signaling and examined glutamine uptake in B cells. This compound has been widely used for specifically inhibiting

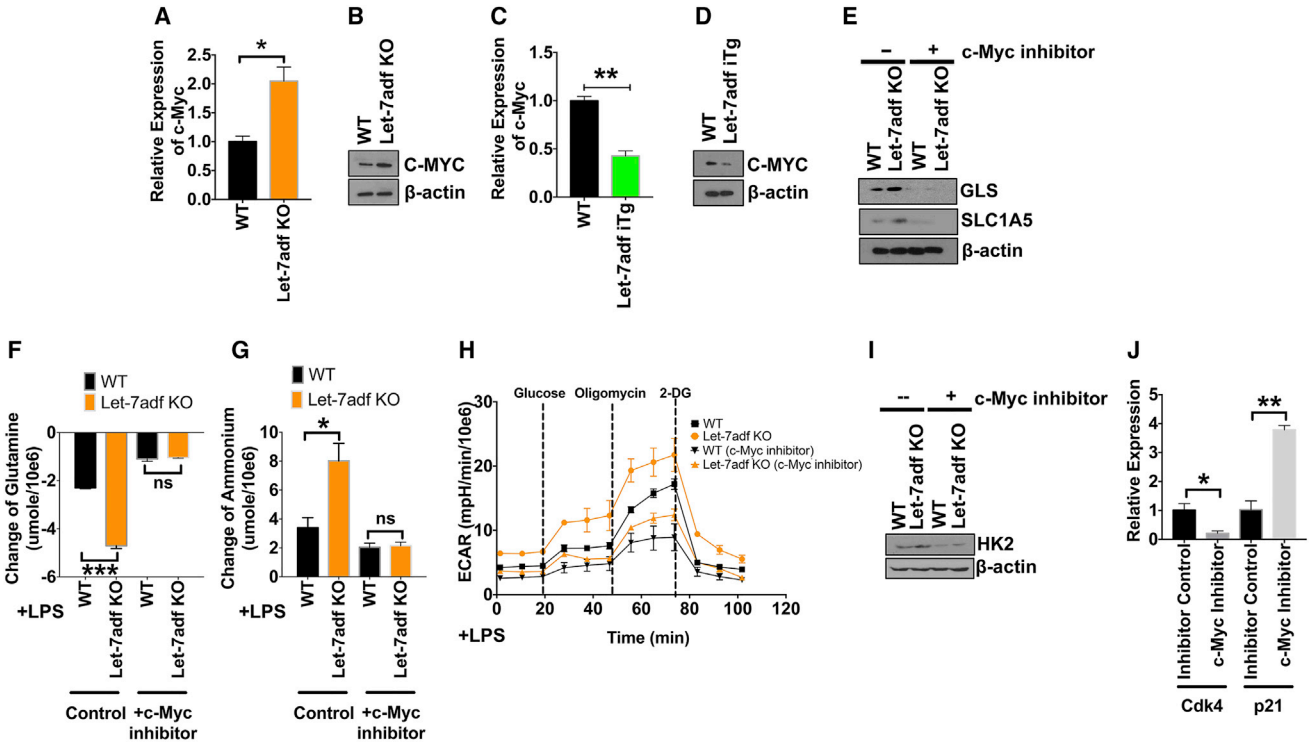

Figure 6. The let-7a-1/let-7d/let-7f-1 Cluster Represses Glutamine Uptake and Utilization by Targeting c-Myc in B Cells

(A) mRNA expression determined by qRT-PCR of c-Myc in WT control or the let-7adf cluster KO B cells.

(B) c-Myc protein expression in B cells from WT or the let-7adf cluster KO mice determined by western blot.

(C) The mRNA expression of c-Myc in WT control or the let-7adf cluster iTg B cells.

(D) c-Myc protein expression in B cells from WT or the let-7adf cluster iTg mice determined by western blot.

(E) Gls and Slc1a5 protein expressions in B cells from WT or the let-7adf cluster KO mice treated by c-Myc inhibitor determined by western blot.

(F) Quantification of glutamine level in c-Myc inhibitor-treated WT or the let-7adf cluster KO B cells activated by LPS.

(G) Quantification of ammonium level in c-Myc inhibitor-treated WT or the let-7adf cluster KO B cells activated by LPS.

(H) Purified the let-7adf cluster KO and WT B cells were treated with c-Myc inhibitor or control and they were examined after 6 hr culture with LPS, and ECAR was determined by extracellular flux analysis. Representative plot of ECAR over time of B cells with addition of glucose (10 mM), oligomycin (1 mM), and 2-DG (20 mM), as indicated.

(I) Hk2 protein expression in either c-Myc inhibitor-treated or control-treated B cells from the let-7adf cluster KO mice or WT control mice obtained by western blot.

(J) mRNA expression determined by qRT-PCR of CDK4 and p21 in c-Myc inhibitor-treated or control-treated B cells.

*$p < 0.05$ and **$p < 0.01$ using Student's t test.

c-Myc in cells (Lucas et al., 2015; Muller et al., 2014; Wang et al., 2014; Zirath et al., 2013). We found that c-Myc inhibition blocked the let-7adf cluster's regulatory effects on the expression of Slc1a5 and Gls (Figure 6E), and on glutaminolysis, indicated by comparable levels of glutamine consumption and ammonium production in B cells (Figures 6F and 6G). We examined glycolysis as measured by the ECAR assay in the presence of the c-Myc inhibitor 10058-F4. We found that let-7adf KO B cells still exhibited higher ECAR compared with the WT control, although c-Myc inhibition suppressed ECAR in both cell lines (Figures 6H and 6I), indicating that the suppression of c-Myc by the let-7adf cluster in stimulated B cells only leads to repressing glutamine uptake and utilization. The altered expression of canonical c-Myc target genes, including Cdk4 and p21 (Figure 6J), further confirmed the effects of c-Myc inhibitor 10058-F4 in B cells. Collectively, these results indicate that the let-7adf cluster represses the uptake and utilization of glutamine by regulating *c-Myc* in B cells.

We next examined whether the observed effects of let-7adf cluster were limited to IgM production. We measured IgG2b and IgG3 production after LPS stimulation in B cells. We found that IgG2b and IgG3 production were higher in let-7adf KO B cells after LPS stimulation, compared with WT B cells (Figures S5A and S5B). In contrast, IgG2b and IgG3 production were lower in let-7adf iTg after LPS stimulation, compared with the WT B cells (Figures S5C and S5D), suggesting that the effect of let-7adf is indeed not limited to IgM production *in vitro*.

Also, we examined if these let-7adf transgenic or KO mice displayed effects on homeostatic antibody production. We did not observe any difference of total serum IgM levels in let-7adf iTg or KO mice compared with their WT controls (Figures S5E and S5F), indicating that the let-7adf cluster is not regulating homeostatic antibody production in mice.

To further examine the possibility that the metabolic effects observed above were the result of changes in B cell populations, we quantitated innate B cells, including marginal zone (MZ) and

B-1 B cell populations, in let-7adf KO mice and found no alterations in frequencies, compared with WT mice (Figures S6A and S6B). Thus, altered frequencies of MZ B cells and B1 B cells do not account for the metabolic changes between let-7adf KO and WT B cells.

DISCUSSION

Metabolic alterations during activation of immune cells such as B cells has recently been drawing attention (Pearce and Pearce, 2013). Activation of B cells requires critical nutrients to build new biomass and to play functional roles during proliferation and antibody production (Caro-Maldonado et al., 2014; Wolowczuk et al., 2008). Most previous work has concentrated on the alterations of metabolism needed to support B cell activation. Thus, we were intrigued to find that let-7 miRNAs play an inhibitory role on B cell activation that involves limiting the metabolic response to activators. In other aspects of immune cell biology, miRNAs play a role of limiting activation processes to avoid autoimmunity and stem cell exhaustion (Mehta and Baltimore, 2016; O'Connell et al., 2010; So et al., 2013).

In the present study, we demonstrate that the let-7adf cluster suppresses antibody production by blocking the uptake and utilization of necessary nutrients including glucose and glutamine. We use several engineered mouse models with gain-of-function and loss-of-function to investigate the role of the let-7 cluster in B cells. We show that the let-7adf cluster restrains glycolytic capacity without significantly influencing mitochondrial respiration in B cells. We could show that *Hk2* is a direct target of the let-7adf cluster and that an HK2 increase promotes B cell glycolysis. The let-7adf cluster curbs B cell glutamine uptake and utilization through regulating glutamine transporter *Slc1a5* and *Gls*, by modulating *c-Myc* in B cells. Our results reveal a novel role for the single let-7adf cluster in the B cell activation by regulation of nutrient uptake and utilization. The let-7adf cluster appears to play a role as a "metabolic brake" during antibody production.

It had been thought that the let-7 family of miRNAs might display functional redundancy due to the high similarity of their seed sequences, which would make it difficult to identify any phenotype associated with an individual let-7 cluster. Whether the multiple let-7 clusters represent a gene redundancy or contribute to different functions in different cellular contexts remains to be fully addressed. In support of a contextual role of individual let-7 gene clusters, liver cell-specific loss of the let-7bc cluster is sufficient to enhance liver regeneration in mice (Nguyen et al., 2014). Conditional depletion of the let-7bc cluster in mouse intestines promotes tumorigenesis of the intestinal epithelium (Madison et al., 2013). Furthermore, emerging evidence indicates that certain single let-7 family members play individual roles in different types of immune cells. For example, let-7f modulates macrophage immune response to infection by *Mycobacterium tuberculosis* through repressing A20 (Kumar et al., 2015), whereas let-7a plays a pro-inflammatory role in an experimental asthma model by targeting IL-13 (Kumar et al., 2011).

In mammals, the functional roles of let-7 have been investigated mainly in the context of cancer. Despite the abundance of the let-7 family in most somatic cells, little is known about their physiological roles in normal tissues, including B cells. This is mainly because of the technical difficulties of examining all let-7 miRNA genes encoded by the eight different genomic loci in loss-of-function studies. Unlike mature let-7, which is undetectable in early embryos and embryonic stem cells, but becomes highly expressed in most adult tissues, the RNA binding protein Lin28a is abundantly expressed in stem cells and cancer cells, and binds to the loop region of pri-let-7 and pre-let-7 miRNA transcripts to inhibit their processing into mature let-7 as well as to facilitate their degradation. Therefore, let-7 repression is commonly seen as a consequence of Lin28a overexpression (Jiang and Baltimore, 2016; Papaioannou et al., 2013; Schulman et al., 2005; Shyh-Chang and Daley, 2013), and Lin28a overexpression has provided a novel way to suppress the endogenous levels of all let-7 family members. Our data show that while Lin28a overexpression affected both TD and TI antigen-induced IgM production, deletion of the let-7adf cluster only altered TI antigen-induced IgM, suggesting that the let-7-independent functions of Lin28a may contribute to the observed phenotype in response to TD antigen challenge. Indeed, it has been reported that Lin28a protein binds to various mRNAs and regulates their translation (Jiang and Baltimore, 2016; Nguyen et al., 2014; Zhu et al., 2011), although the physiological significance of these findings remains to be determined in future studies. However, it is also possible that other let-7 clusters, although not the let-7bc cluster, might contribute to control of antibody synthesis.

We are able to show that the let-7adf cluster, but not the let-7bc cluster, influenced TI antigen-induced IgM production in both loss- and gain-of-function engineered mouse models. The role of single let-7 clusters had not been previously studied in B cells. Thus, the identified mechanism by which the let-7adf cluster suppresses both glycolysis and glutaminolysis broadens our understanding of the role of let-7 members in B cells.

Emerging evidence demonstrates that increased glycolysis and glutaminolysis are part of a metabolic switch during B cell activation (Caro-Maldonado et al., 2014; Le et al., 2012). How these two key metabolic nutrients are regulated in a synchronized manner to maintain defined levels of the building blocks and energy needed for antibody production remained unclear, and our studies indicate a critical modulating role of the let-7adf cluster in this process.

We do not fully understand the physiological or pathological roles of let-7 clusters in the immune system, but it is clear that the let-7adf cluster acts as a negative regulator of antibody production, perhaps to avoid pathology, perhaps to give the system an unused capability that would be available in an emergency. To more deeply understand the cluster's physiological or pathological role in B cells, however, will require long-term monitoring of aging let-7adf cluster KO mice, which we hope to examine in the future.

Collectively, in this study we showed the significance of the let-7adf cluster in the regulation of IgM production in B cells using engineered murine models. These findings reveal a central role for the single let-7adf cluster in the regulation of B cell metabolic processes.

Limitations of Study

The activation of small B lymphocytes from a quiescent state into large, dividing, and antibody-secreting cells involves major

alterations in the metabolism of the cells. We show here that a miRNA cluster plays a critical role in limiting the extent of this cellular transition, but many questions remain unanswered. In particular, we can only guess at the physiological role of the let-7-induced events. Because we have found that other miRNA-mediated processes can best be appreciated in the context of the aging mouse, it could well be that let-7's inhibitory role can be understood by knocking out the let-7adf cluster selectively in the B cell compartment and then following the behavior of B cells over the 2-year lifespan of the mice. Also, our work only relates to the adf cluster, not all of the let-7 clusters and isoforms. It also relates specifically to TI activation of B cells and not the more common TD process. There may also be other miRNAs that play similar roles. It would be significant to know how widespread miRNA-mediated control of metabolism might be and how it evolved to play its roles. Finally, the possible clinical roles that miRNAs might play in immune pathology can only be understood by knowing the roles that these RNAs play in immune cell physiology.

STAR★METHODS

Detailed methods are provided in the online version of this paper and include the following:

- KEY RESOURCES TABLE
- CONTACT FOR REAGENT AND RESOURCE SHARING
- EXPERIMENTAL MODEL AND SUBJECT DETAILS
  - Mouse Studies
  - Cell Cultures
- METHOD DETAILS
  - Mice
  - Western Blot
  - RNA Extraction and RT Real-Time qPCR
  - DNA Constructs
  - Luciferase Reporter Assays
  - B Cell Isolation
  - Flow Cytometry
  - Seahorse Analyzer
  - Sample Preparation for NMR Spectroscopy and NMR Experiments
  - Immunizations and ELISAs
  - Medium Metabolite Analysis
  - Measurements of Metabolite Levels Using Commercial Kits
- QUANTIFICATION AND STATISTICAL ANALYSIS

SUPPLEMENTAL INFORMATION

Supplemental Information includes six figures and can be found with this article online at https://doi.org/10.1016/j.cmet.2017.12.007.

ACKNOWLEDGMENTS

We are grateful to Drs. George Daley (Harvard Medical School), Antony Rodriguez, Eric Olson (University of Texas Southwestern Medical Center), and Tatsuya Kobayashi (Massachusetts General Hospital) for providing the iTg and KO mice. We thank Dr. Yuan Chen at City of Hope Nuclear Magnetic Resonance (NMR) Core facility for assistance with our NMR experimental training. This study is supported by the NIH grants R01AI079243 (D.B.), R01CA163586 (S.E.W.), and R01CA166020 (S.E.W.).

AUTHOR CONTRIBUTIONS

S.J., W.Y., S.E.W., and D.B. designed research; S.J. and W.Y. performed research; S.J. and W.Y. analyzed data; and S.J., W.Y., S.E.W., and D.B. wrote the paper.

Received: April 12, 2017
Revised: July 19, 2017
Accepted: December 9, 2017
Published: January 11, 2018

REFERENCES

Agarwal, V., Bell, G.W., Nam, J.W., and Bartel, D.P. (2015). Predicting effective microRNA target sites in mammalian mRNAs. Elife *4*, e05005.

Baltimore, D., Boldin, M.P., O'Connell, R.M., Rao, D.S., and Taganov, K.D. (2008). MicroRNAs: new regulators of immune cell development and function. Nat. Immunol. *9*, 839–845.

Boyerinas, B., Park, S.M., Hau, A., Murmann, A.E., and Peter, M.E. (2010). The role of let-7 in cell differentiation and cancer. Endocr. Relat. Cancer *17*, F19–F36.

Buck, M.D., O'Sullivan, D., and Pearce, E.L. (2015). T cell metabolism drives immunity. J. Exp. Med. *212*, 1345–1360.

Calder, P.C. (2006). Branched-chain amino acids and immunity. J. Nutr. *136*, 288S–293S.

Capasso, M., Rashed Alyahyawi, A., and Spear, S. (2015). Metabolic control of B cells: more questions than answers. Front. Immunol. *6*, 80.

Caro-Maldonado, A., Wang, R., Nichols, A.G., Kuraoka, M., Milasta, S., Sun, L.D., Gavin, A.L., Abel, E.D., Kelsoe, G., Green, D.R., and Rathmell, J.C. (2014). Metabolic reprogramming is required for antibody production that is suppressed in anergic but exaggerated in chronically BAFF-exposed B cells. J. Immunol. *192*, 3626–3636.

Doughty, C.A., Bleiman, B.F., Wagner, D.J., Dufort, F.J., Mataraza, J.M., Roberts, M.F., and Chiles, T.C. (2006). Antigen receptor-mediated changes in glucose metabolism in B lymphocytes: role of phosphatidylinositol 3-kinase signaling in the glycolytic control of growth. Blood *107*, 4458–4465.

Dubinsky, A.N., Dastidar, S.G., Hsu, C.L., Zahra, R., Djakovic, S.N., Duarte, S., Esau, C.C., Spencer, B., Ashe, T.D., Fischer, K.M., et al. (2014). Let-7 coordinately suppresses components of the amino acid sensing pathway to repress mTORC1 and induce autophagy. Cell Metab. *20*, 626–638.

Dufort, F.J., Bleiman, B.F., Gumina, M.R., Blair, D., Wagner, D.J., Roberts, M.F., Abu-Amer, Y., and Chiles, T.C. (2007). Cutting edge: IL-4-mediated protection of primary B lymphocytes from apoptosis via Stat6-dependent regulation of glycolytic metabolism. J. Immunol. *179*, 4953–4957.

Esquela-Kerscher, A., Trang, P., Wiggins, J.F., Patrawala, L., Cheng, A., Ford, L., Weidhaas, J.B., Brown, D., Bader, A.G., and Slack, F.J. (2008). The let-7 microRNA reduces tumor growth in mouse models of lung cancer. Cell Cycle *7*, 759–764.

Fong, M.Y., Zhou, W., Liu, L., Alontaga, A.Y., Chandra, M., Ashby, J., Chow, A., O'Connor, S.T., Li, S., Chin, A.R., et al. (2015). Breast-cancer-secreted miR-122 reprograms glucose metabolism in premetastatic niche to promote metastasis. Nat. Cell Biol. *17*, 183–194.

Gao, P., Tchernyshyov, I., Chang, T.C., Lee, Y.S., Kita, K., Ochi, T., Zeller, K.I., De Marzo, A.M., Van Eyk, J.E., Mendell, J.T., and Dang, C.V. (2009). c-Myc suppression of miR-23a/b enhances mitochondrial glutaminase expression and glutamine metabolism. Nature *458*, 762–765.

Grohmann, U., and Bronte, V. (2010). Control of immune response by amino acid metabolism. Immunol. Rev. *236*, 243–264.

Hensley, C.T., Wasti, A.T., and DeBerardinis, R.J. (2013). Glutamine and cancer: cell biology, physiology, and clinical opportunities. J. Clin. Invest. *123*, 3678–3684.

Hu, X., Guo, J., Zheng, L., Li, C., Zheng, T.M., Tanyi, J.L., Liang, S., Benedetto, C., Mitidieri, M., Katsaros, D., et al. (2013). The heterochronic microRNA let-7 inhibits cell motility by regulating the genes in the actin cytoskeleton pathway in breast cancer. Mol. Cancer Res. *11*, 240–250.

Jiang, S., and Baltimore, D. (2016). RNA-binding protein Lin28 in cancer and immunity. Cancer Lett. *375*, 108–113.

Kolenda, T., Przybyła, W., Teresiak, A., Mackiewicz, A., and Lamperska, K.M. (2014). The mystery of let-7d - a small RNA with great power. Contemp. Oncol. (Pozn.) *18*, 293–301.

Kumar, M., Ahmad, T., Sharma, A., Mabalirajan, U., Kulshreshtha, A., Agrawal, A., and Ghosh, B. (2011). Let-7 microRNA-mediated regulation of IL-13 and allergic airway inflammation. J. Allergy Clin. Immunol. *128*, 1077–1085.e1-10.

Kumar, M., Sahu, S.K., Kumar, R., Subuddhi, A., Maji, R.K., Jana, K., Gupta, P., Raffetseder, J., Lerm, M., Ghosh, Z., et al. (2015). MicroRNA let-7 modulates the immune response to *Mycobacterium tuberculosis* infection via control of A20, an inhibitor of the NF-κB pathway. Cell Host Microbe *17*, 345–356.

Le, A., Lane, A.N., Hamaker, M., Bose, S., Gouw, A., Barbi, J., Tsukamoto, T., Rojas, C.J., Slusher, B.S., Zhang, H., et al. (2012). Glucose-independent glutamine metabolism via TCA cycling for proliferation and survival in B cells. Cell Metab. *15*, 110–121.

Lucas, C.M., Harris, R.J., Giannoudis, A., and Clark, R.E. (2015). c-Myc inhibition decreases CIP2A and reduces BCR-ABL1 tyrosine kinase activity in chronic myeloid leukemia. Haematologica *100*, e179–182.

Madison, B.B., Liu, Q., Zhong, X., Hahn, C.M., Lin, N., Emmett, M.J., Stanger, B.Z., Lee, J.S., and Rustgi, A.K. (2013). LIN28B promotes growth and tumorigenesis of the intestinal epithelium via Let-7. Genes Dev. *27*, 2233–2245.

Mathupala, S.P., Ko, Y.H., and Pedersen, P.L. (2006). Hexokinase II: cancer's double-edged sword acting as both facilitator and gatekeeper of malignancy when bound to mitochondria. Oncogene *25*, 4777–4786.

Mehta, A., and Baltimore, D. (2016). MicroRNAs as regulatory elements in immune system logic. Nat. Rev. Immunol. *16*, 279–294.

Muller, I., Larsson, K., Frenzel, A., Oliynyk, G., Zirath, H., Prochownik, E.V., Westwood, N.J., and Henriksson, M.A. (2014). Targeting of the MYCN protein with small molecule c-MYC inhibitors. PLoS One *9*, e97285.

Nakaya, M., Xiao, Y., Zhou, X., Chang, J.H., Chang, M., Cheng, X., Blonska, M., Lin, X., and Sun, S.C. (2014). Inflammatory T cell responses rely on amino acid transporter ASCT2 facilitation of glutamine uptake and mTORC1 kinase activation. Immunity *40*, 692–705.

Nguyen, L.H., Robinton, D.A., Seligson, M.T., Wu, L., Li, L., Rakheja, D., Comerford, S.A., Ramezani, S., Sun, X., Parikh, M.S., et al. (2014). Lin28b is sufficient to drive liver cancer and necessary for its maintenance in murine models. Cancer Cell *26*, 248–261.

Nguyen, L.H., and Zhu, H. (2015). Lin28 and let-7 in cell metabolism and cancer. Transl. Pediatr. *4*, 4–11.

O'Connell, R.M., Rao, D.S., Chaudhuri, A.A., and Baltimore, D. (2010). Physiological and pathological roles for microRNAs in the immune system. Nat. Rev. Immunol. *10*, 111–122.

Papaioannou, G., Inloes, J.B., Nakamura, Y., Paltrinieri, E., and Kobayashi, T. (2013). let-7 and miR-140 microRNAs coordinately regulate skeletal development. Proc. Natl. Acad. Sci. USA *110*, E3291–E3300.

Pearce, E.L., and Pearce, E.J. (2013). Metabolic pathways in immune cell activation and quiescence. Immunity *38*, 633–643.

Reinhart, B.J., Slack, F.J., Basson, M., Pasquinelli, A.E., Bettinger, J.C., Rougvie, A.E., Horvitz, H.R., and Ruvkun, G. (2000). The 21-nucleotide let-7 RNA regulates developmental timing in *Caenorhabditis elegans*. Nature *403*, 901–906.

Rottiers, V., and Naar, A.M. (2012). MicroRNAs in metabolism and metabolic disorders. Nat. Rev. Mol. Cell Biol. *13*, 239–250.

Sampson, V.B., Rong, N.H., Han, J., Yang, Q., Aris, V., Soteropoulos, P., Petrelli, N.J., Dunn, S.P., and Krueger, L.J. (2007). MicroRNA let-7a down-regulates MYC and reverts MYC-induced growth in Burkitt lymphoma cells. Cancer Res. *67*, 9762–9770.

Schulman, B.R., Esquela-Kerscher, A., and Slack, F.J. (2005). Reciprocal expression of lin-41 and the microRNAs let-7 and mir-125 during mouse embryogenesis. Dev. Dyn. *234*, 1046–1054.

Shotwell, M.A., Kilberg, M.S., and Oxender, D.L. (1983). The regulation of neutral amino acid transport in mammalian cells. Biochim. Biophys. Acta *737*, 267–284.

Shyh-Chang, N., and Daley, G.Q. (2013). Lin28: primal regulator of growth and metabolism in stem cells. Cell Stem Cell *12*, 395–406.

Shyh-Chang, N., Zhu, H., Yvanka de Soysa, T., Shinoda, G., Seligson, M.T., Tsanov, K.M., Nguyen, L., Asara, J.M., Cantley, L.C., and Daley, G.Q. (2013). Lin28 enhances tissue repair by reprogramming cellular metabolism. Cell *155*, 778–792.

So, A.Y., Zhao, J.L., and Baltimore, D. (2013). The Yin and Yang of microRNAs: leukemia and immunity. Immunol. Rev. *253*, 129–145.

Su, J.L., Chen, P.S., Johansson, G., and Kuo, M.L. (2012). Function and regulation of let-7 family microRNAs. MicroRNA *1*, 34–39.

Wagner, S., Ngezahayo, A., Murua Escobar, H., and Nolte, I. (2014). Role of miRNA let-7 and its major targets in prostate cancer. Biomed. Res. Int. *2014*, 376326.

Wang, J., Ma, X., Jones, H.M., Chan, L.L., Song, F., Zhang, W., Bae-Jump, V.L., and Zhou, C. (2014). Evaluation of the antitumor effects of c-Myc-Max heterodimerization inhibitor 100258-F4 in ovarian cancer cells. J. Transl. Med. *12*, 226.

Wang, X., Cao, L., Wang, Y., Wang, X., Liu, N., and You, Y. (2012). Regulation of let-7 and its target oncogenes (Review). Oncol. Lett. *3*, 955–960.

Wang, Z., Lin, S., Li, J.J., Xu, Z., Yao, H., Zhu, X., Xie, D., Shen, Z., Sze, J., Li, K., et al. (2011). MYC protein inhibits transcription of the microRNA cluster MC-let-7a-1∼let-7d via noncanonical E-box. J. Biol. Chem. *286*, 39703–39714.

Wolowczuk, I., Verwaerde, C., Viltart, O., Delanoye, A., Delacre, M., Pot, B., and Grangette, C. (2008). Feeding our immune system: impact on metabolism. Clin. Dev. Immunol. *2008*, 639803.

Woodland, R.T., Fox, C.J., Schmidt, M.R., Hammerman, P.S., Opferman, J.T., Korsmeyer, S.J., Hilbert, D.M., and Thompson, C.B. (2008). Multiple signaling pathways promote B lymphocyte stimulator dependent B-cell growth and survival. Blood *111*, 750–760.

Wu, L., Nguyen, L.H., Zhou, K., de Soysa, T.Y., Li, L., Miller, J.B., Tian, J., Locker, J., Zhang, S., Shinoda, G., et al. (2015). Precise let-7 expression levels balance organ regeneration against tumor suppression. Elife *4*, e09431.

Zhu, H., Shyh-Chang, N., Segre, A.V., Shinoda, G., Shah, S.P., Einhorn, W.S., Takeuchi, A., Engreitz, J.M., Hagan, J.P., Kharas, M.G., et al. (2011). The Lin28/let-7 axis regulates glucose metabolism. Cell *147*, 81–94.

Zirath, H., Frenzel, A., Oliynyk, G., Segerstrom, L., Westermark, U.K., Larsson, K., Munksgaard Persson, M., Hultenby, K., Lehtio, J., Einvik, C., et al. (2013). MYC inhibition induces metabolic changes leading to accumulation of lipid droplets in tumor cells. Proc. Natl. Acad. Sci. USA *110*, 10258–10263.

STAR★METHODS

KEY RESOURCES TABLE

REAGENT or RESOURCE	SOURCE	IDENTIFIER
Antibodies		
c-Myc	Cell Signaling Technology	5605s; RRID: AB_1903938
Glutaminase (Gls)	Abcam	Ab93434; RRID: AB_10561964
Slc1a5	Santa Cruz Biotechnology	sc-50695; RRID: AB_2190878
Hk2	Cell Signaling Technology	2867; RRID: AB_2232946
Pdk1	Santa Cruz Biotechnology	sc-7140; RRID: AB_2161140
Glut1	Santa Cruz Biotechnology	sc-1603; RRID: AB_2254952
β-actin	Sigma-Aldrich	A3854; RRID: AB_262011
Goat anti-Mouse IgM Antibody Affinity Purified	Bethyl Laboratories	A90-101A; RRID: AB_67186
Goat anti-Mouse IgM Antibody HRP Conjugated	Bethyl Laboratories	A90-101P; RRID: AB_67189
Goat anti-Mouse IgG2b Antibody Affinity Purified	Bethyl Laboratories	A90-109A; RRID: AB_67157
Goat anti-Mouse IgG2b Antibody HRP Conjugated	Bethyl Laboratories	A90-109P; RRID: AB_67160
Goat anti-Mouse IgG3 Antibody Affinity Purified	Bethyl Laboratories	A90-111A; RRID: AB_67167
Goat anti-Mouse IgG3 Antibody HRP Conjugated	Bethyl Laboratories	A90-111P; RRID: AB_67170
Chemicals, Peptides, and Recombinant Proteins		
c-Myc inhibitor 10058-F4	Sigma-Aldrich	F3680
Leaf Purified anti-mouse CD40 Antibody	BioLegend	102908
Lipopolysaccharides from *Escherichia coli* O55:B5	Sigma-Aldrich	L4524
TNP-LPS	Biosearch Technologies	T-5065-5
TNP-AECM-FICOLL	Biosearch Technologies	F-1300-10
Hooke Kit Ovalbumin/CFA Emulsion	Hooke Laboratories	EK-0301
Critical Commercial Assays		
XF Glycolysis Stress Test Kit	Seahorse Bioscience	103020-100
XF Cell Mito Stress Test Kit	Seahorse Bioscience	103015-100
EasySep Mouse B Cell Isolation Kit	StemCell Technologies	19854RF
iScript(tm) Select cDNA Synthesis Kit	Bio-Rad	1708897
Taqman (R) microRNA RT KIT 200 RXNS	Life Technologies	4366596
Taqman Fast Advanced MMIX 5 ML	Life Technologies	4444557
KAPA SYBR FAST Universal	Kapa Biosystems	KK4602
Glucose Assay Kit	Abcam	ab65333
Glutamate-Glo Assay	Promega	J7021
Glutamine Colorimetric Assay Kit	Biovision	K556
EnzyChrom Ammonia/Ammonium Assay Kit	BioAssay Systems	ENH3-100
Dual Luciferase Reporter (DLR) Assay Systems	Fisher Scientific	PRE1941
Experimental Models: Cell Lines		
HEK293T	ATCC	CRL 11268
Experimental Models: Organisms/Strains		
Mouse: Lin28a iTg	Dr. Tatsuya Kobayashi Lab	N/A
Mouse: Let-7adf cluster iTg	Dr. Eric Olson Lab	N/A
Mouse: Let-7adf cluster KO	Dr. George Daley Lab	N/A
Mouse: Let-7bc cluster KO	Dr. George Daley Lab	N/A
Mouse: B6.129P2(C)-Cd19tm1(cre)Cgn/J	The Jackson Laboratory	N/A
Mouse: Lin28a CD19 iTg	This paper	N/A
Mouse: Let-7adf cluster CD19 iTg	This paper	N/A

(*Continued on next page*)

Continued

REAGENT or RESOURCE	SOURCE	IDENTIFIER
Oligonucleotides		
Gls qPCR primers: Forward Primer: 5′-GACTTCTCAGGGCAGTTTGC-3′ Reverse Primer: 5′-TCCTTCTCTCCGAGGATCAA-3′	This paper	N/A
Pdk1 qPCR primers: Forward Primer: 5′-GACTGTGAAGATGAGTGACCG-3′ Reverse Primer: 5′-CAATCCGTAACCAAACCCAG-3′	This paper	N/A
Hk2 qPCR primers: Forward Primer: 5′-GGGTAGCCACGGAGTACAAA-3′ Reverse Primer: 5′-TGGATTGAAAGCCAACTTCC-3′	This paper	N/A
Slc1a5 qPCR primers: Forward Primer: 5′-CCCCTCCTGAAACAGTACCA-3′ Reverse Primer: 5′-AGCCTCTCCAGGAAGGAGAC-3′	This paper	N/A
c-Myc qPCR primers: Forward Primer: 5′-ACACGGAGGAAAACGACAAG-3′ Reverse Primer: 5′-AGAGGTGAGCTTGTGCTCGT-3′	This paper	N/A
Cdk4 qPCR primers: Forward Primer: 5′-CAATGTTGTACGGCTGATGG-3′ Reverse Primer: 5′-CAGGCCGCTTAGAAACTGAC-3′	This paper	N/A
P21 qPCR primers: Forward Primer: 5′-GCCTTAGCCCTCACTCTGTG-3′ Reverse Primer: 5′-AGGGCCCTACCGTCCTACTA-3′	This paper	N/A
β-actin qPCR primers: Forward Primer: 5′ AGGTGTGCACCTTTTATTGGTCTCAA-3′ Reverse Primer: 5′-TGTATGAAGGTTTGGTCTCCCT-3′	This paper	N/A
Recombinant DNA		
psiCHECK-2 HK2 3′ UTR or HK2 3′ UTR mut	This paper	N/A
pBABE-HK2	This paper	N/A
Software and Algorithms		
GraphPad Prism 7	GraphPad Software	http://www.graphpad.com/scientificsoftware/prism/
Chenomx NMR Suite 7.5	Chenomx Software	http://www.chenomx.com/software/
Sparky 3	Sparky Software	https://www.cgl.ucsf.edu/home/sparky/
Other		
RBC Lysis Buffer (10X)	BioLegend	420301
RIPA buffer	Sigma-Aldrich	R0278
Trizol Reagent	Life Technologies	15596018
Lipofectamine RNAiMAX Transfection Reagent	Life Technologies	13778075
MirVana miRNA Mimic, Negative Control	Life Technologies	4464058
Assay Id MC11778 mirVana miRNA Mimic Scale 5 nmol	Life Technologies	4464066

CONTACT FOR REAGENT AND RESOURCE SHARING

Further information and requests for resources and reagents should be directed to and will be fulfilled by the Lead Contact, David Baltimore (baltimo@caltech.edu).

EXPERIMENTAL MODEL AND SUBJECT DETAILS

Mouse Studies

Mice were bred and housed in the animal facility of Caltech. All the animal procedures were carried out in accordance with Institutional Animal Care and Use Committee guidelines. All mice were maintained on standard rodent chow under 12 hr light/ 12 hr dark cycle. All mice in these experiments were in good health.

Cell Cultures

HEK293T cells were cultured in DMEM (4.5g/L glucose) supplemented with 10% FBS at 37°C with 5% CO2. The sex of this cell line was unknown.

METHOD DETAILS

Mice

The cre-inducible Lin28a expression transgenic (Lin28a iTg) mice were a gift from Dr. Tatsuya Kobayashi. The Lin28a iTg mice have been described by Dr. Tatsuya Kobayashi (Massachusetts General Hospital) (Papaioannou et al., 2013). The let-7adf cluster KO mice and the let-7bc cluster KO mice were gifts from Dr. George Daley (Harvard Medical School) and Dr. Antony Rodriguez. The let-7adf cluster iTg mice were a gift from Dr. Eric Olson (University of Texas Southwestern Medical Center).

Western Blot

Total purified B cell extracts were analyzed by electrophoresis on a 10%-12% SDS polyacrylamide gel. Protein detection was performed using the antibodies listed in the Key Resources Table.

RNA Extraction and RT Real-Time qPCR

RNA was isolated by TRIzol (Invitrogen) as per the manufacturer's instructions. We performed SYBR Green-based (Bio-Rad) quantitative real-time PCR with an Eppendorf Real-Time PCR machine to assay mRNA levels. A Taqman approach was used to quantify let-7 and snoRNA-202 expressions (Applied Biosystems). All mRNA levels were normalized to β-actin, whereas let-7 levels were normalized to snoRNA-202. We performed SYBR Green–based RT-qPCR for mRNA expression of mouse Hk2, Pdk1, c-Myc, Slc1a5, Gls, Cdk4 and p21 after cDNA synthesis using iScript Select cDNA Synthesis Kit (Bio-Rad) and detection with KAPA SYBR FAST Universal (KAPA BIOSYSTEMS INC) as per manufacturer's instructions. Sequence-specific primers for qPCR are listed in the Key Resources Table.

DNA Constructs

For HK2 rescue experiments, the *HK2* cDNA was cloned into the pBABE-Puro retroviral vector as previously described (Fong et al., 2015). For luciferase assays, the PCR-amplified *Hk2* 3′ UTR or a Hk2 3′ UTR with a mutant miR-let-7d–binding site were cloned into the psiCHECK-2 reporter vector as previously described (Fong et al., 2015).

Luciferase Reporter Assays

HEK293T cells were co-transfected with either let-7d mimics or negative control (Ambion), and psiCHECK-2 reporting vector containing either the Hk2 3′ UTR, or a Hk2 3′ UTR with a mutant miR-let-7d–binding site. Cells were harvested 48 hr after transfection. Luciferase activity was measured using The Dual-luciferase Reporter Assay System (Promega) and normalized to respective controls.

B Cell Isolation

Splenic naive B were isolated by B cell isolation kit (Purity was typically above 90%; Stem Cell Technology) and cultured in RPMI 1640 supplemented with 10% FBS. For *in vitro* studies, purified B cells were stimulated with either anti-CD40 (5μg/ml) or LPS (10ug/ml) for 7 days. Supernatant were collected on day 7. Antibody secretion was analyzed by ELISA assays.

Flow Cytometry

Relevant tissues were harvested and cells were homogenized and subsequently depleted of red blood cells. Flurophore-conjugated antibodies were used for the indicated markers, and detected using a MACSQuant10 Flow Cytometry machine (Miltenyi).

Seahorse Analyzer

Oxygen consumption rate (OCR) and extracellular acidification rate (ECAR) were measured with an XF^e24 extracellular flux analyzer (Seahorse Bioscience). Briefly, $1.4e^6$ unstimulated or $1.4e^6$ LPS-stimulated cells/well of purified B cells were seeded in a 24 well plate, and OCR and ECAR measurements were normalized to cell number. Cells were initially plated in XF^e Seahorse media with 2mM glutamine in ECAR tests, or 10mM glucose and 2mM glutamine, 1mM Sodium pyruvate in mitochondrial stress test using the following concentrations of injected compounds, as indicated in the text: oligomycin, 1μM; rotenone, 0.75μM; electron transport chain accelerator p-trifluoromethoxy carbonyl cyanide phenyl hydrazine (FCCP), 0.5μM; antimycin A, 1.5μM; 2-DG, 50mM; glucose, 10mM.

Sample Preparation for NMR Spectroscopy and NMR Experiments

The metabolites in the LPS-treated B cells were measured using NMR spectroscopy. Sample preparation, for ^{13}C-glucose labeling, briefly, B cells were cultured with 16.6mM (3g/L) D-$^{13}C_6$ glucose (Aldrich) for 6 hr; for ^{13}C-glutamine labeling, B cells were cultured with 4mM L-glutamine-$^{13}C_5$ (Aldrich) for 6 hr. After weight, the harvested samples were resuspended in 7.4ml/g pre-cold methanol and 2.22ml/g pre-cold water; After sonication (25% duty cycle), add 3.7ml/g cold chloroform and kept at 4°C overnight. Add 3.7ml/g chloroform and 3.7ml/g H_2O addition followed by that the solutions were vortexed and centrifuged for 5 min on the next day. The

upper hydrophilic layer was dried in a speed-vac concentrator. Hydrophilic samples dried from the methanol-water fractions were each resuspended in 500μl Deuterium Oxide "100%" (D, 99.96%) (D_2O) containing 5μM (One-dimensional NMR spectra, 1D) or 5mM (Two-dimensional NMR spectra, 2D) Sodium 2,2-Dimethyl-2-Silapentane-5-Sulfonate (DSS) (Cambridge Isotope Laboratories, MA), which serves as an internal chemical shift reference and a concentration standard. One-dimensional NMR spectra were acquired at 25°C on a Bruker Avance spectrometer equipped with a cryoprobe operating at 600.19 MHz ^{1}H frequency. Pre-saturation was used to suppress water signal, and the spectra were collected with spectral width of 10kHz, 32k data points, 3s relaxation delay and 1,024 transients. The data were processed using Bruker topspin 3.1, and analyzed using Chenomix software (version 7.5, Chenomx). Two-dimensional NMR spectra were acquired at 25°C on a Bruker Avance spectrometer equipped with a cryoprobe operating at 600.19 MHz ^{1}H frequency. The spectrum width for ^{1}H and ^{13}C are 16.0208 ppm and 13.9778 ppm, respectively. The acquisition time for ^{1}H and ^{13}C are 3.4079740 and 0.1221704s, respectively. ^{1}H ^{13}C NMR spectra of the samples were processed using Bruker topspin 3.1, and analyzed using Sparky software.

Immunizations and ELISAs

Engineered mice were immunized by i.p. injection with OVA-CFA or TNP-Ficoll or TNP-LPS. For T cell-independent responses, sera from 8-12 weeks old mice were collected at day 0 and day 7 after i.p. injection of 50ug TNP-Ficoll or 50ug TNP-LPS. TNP-specific IgM was examined by ELISA assays. For T cell-dependent responses, mice were immunized subcutaneously with 50ug OVA/CFA, and sera from 8-12 weeks old mice were collected at day 0 and day 21 after i.p. injection of 50ug OVA/CFA. OVA specific-IgM was examined by ELISA assay.

Medium Metabolite Analysis

Purified B cells seeded at equal number were cultured in growth medium treated with LPS (10ug/ml) for 24 hr before medium was collected, cleared by centrifugation, and subjected to metabolite measurement using a BioProfile 100 Plus (Nova Biomedical) as previously described (Fong et al., 2015). Medium collected from cell-free plates after 24h incubation was used as the baseline control to calculate the consumption or production of each metabolite, which was further normalized to the cell number in each plate determined at the time of medium collection.

Measurements of Metabolite Levels Using Commercial Kits

Metabolites were measured by commercial kits: Glucose assay kit (Abcam), Glutamate-Glo assay kit (Promega), Glutamine colourimetric assay kit (BioVision), and EnzyChrom ammonia/ammonium assay kit (BioAssay Systems).

QUANTIFICATION AND STATISTICAL ANALYSIS

All statistical analysis was done in GraphPad Prism 7 software using an unpaired Student's t test. Data were reported as mean ± SEM. Significance measurements were marked as follows: *$p < 0.05$, **$p < 0.01$, ***$p < 0.001$, or ns for not significant. Statistical details of experiments can be found in the figure legends.